Microstructure, transformation behavior and mechanical properties of a $(Ti_{50}Ni_{38}Cu_{12})_{93}Nb_7$ alloy

Daqaing Jiang[1, 2, *], Yinong Liu[1], Weilong Liu[2], Lixie Song[2], Xiaohua Jiang[2], Hong Yang[1], Lishan Cui[2]

[1]School of Mechanical and Chemical Engineering, The University of Western Australia, Australia

[2]Department of Materials Science and Engineering, China University of Petroleum - Beijing, China

[*]To whom correspondence should be addressed. E-mail: daqiang.jiang@uwa.edu.au.

Tel: 86-10-89733975; Fax: 86-10-89731959

Abstract: A $(Ti_{50}Ni_{38}Cu_{12})_{93}Nb_7$ alloy is fabricated by arc melting, forging and drawing. The microstructure, transformation behavior and mechanical properties were investigated by means of scanning electron microscope (SEM), differential scanning calorimeter (DSC), dynamic mechanical analyzer (DMA) and tensile test machine. SEM observation showed that the as cast alloy is composed of TiNiCu and Nb-rich phases. After drawing, the alloy showed single step transformations during heating and cooling within the whole annealing temperature range from 400 °C to 800 °C. With the increase of the annealing temperature, both the transformation temperatures and the damping capacity increased first and then decreased. The ultimate strength of the alloy after annealing at 400 °C is over 1500 MPa and the maximum elongation of the alloy after annealing at 800 °C is more than 20%.

Key words: Shape memory alloy; Martensitic transformation; Mechanical property

1. Introduction

The substitution of Cu for Ni in binary TiNi shape memory alloy (SMA) has been shown to change the transformation behavior. TiNiCu alloys with Cu content of more than 7.5 at.% showed the B2-B19-B19’ or the B2-B19 transformation behavior [1]. The shape memory characteristics associated with the B2-B19 transformation in TiNiCu alloys were very attractive for many industrial applications because these characteristics lay in-between those of the B2-R and B2-B19’ transformations in TiNi SMAs, and showed a better combination of relatively larger transformation strain (2.5-3.2%) than that (~1%) of B2-R and smaller hysteresis (4-20K) than that (~60K) of B2-B19’ [1, 2]. Unfortunately, TiNiCu alloys with Cu content of more than 10 at.% are so brittle that plastic deformation is not possible [3].

Therefore, it is desirable to develop new alloys which show the B2-B19 transformation and good workability.

There have been some works on adding the fourth element into the TiNiCu SMA to suppress the B2-B19' transformation, such as Mo, Cr, and Fe et al. [4-6]. It is known that the Nb element can suppress the B2-B19' transformation in TiNi alloy [7, 8] and can improve the cold workability due to the formation of a ductile Nb-rich phase in TiNiHf alloy [9]. Moreover, according to the binary Cu-Nb phase diagram [10], there is no brittle intermetallic compound formed at high temperature and the two elements were immiscible at room temperature. Therefore, the cold workability and transformation behavior of the TiNiCu alloy are expected to be improved if the Nb element was added into the TiNiCu alloy. However, up to now there has been no report on TiNiCuNb shape memory alloys containing a ductile phase. In this study, a new TiNiCuNb alloy was designed and the microstructure, transformation behavior and mechanical properties were investigated.

2. Experimental procedure

2.1 Material preparation

An ingot of 0.5 kg with composition of $(Ti_{50}Ni_{38}Cu_{12})_{93}Nb_7$ was produced from high-purity elemental metals of the constituents (purity >99.8 wt. %) by arc melting. The ingot was hot-forged at 800 °C and further hot-drawn at 500 °C into a thick wire of 2 mm in diameter. Then the hot-drawn wire was cold-drawn into a thin wire of 0.5 mm in diameter at room temperature with intermediate annealing at 630 °C. The samples for transformation behavior and mechanical test were cut from the cold-drawn wire and were subsequently annealed at different temperatures for 20 min followed by air cooling.

2.2 Characterization

A FEI Quanta 200F scanning electron microscope (SEM) was used for microstructure characterization. The phase component was characterized by means of x-ray diffraction (XRD, Bruker AXS D8) using Cu Kα radiation. Transformation behaviors were characterized by using TA Q20 differential scanning calorimeter (DSC) with a heating/cooling rate of 10 °C/min. A TA Q800 instrument was used to record the Tan Delta (Q^{-1})-temperature curves of the samples with a heating rate of 3 °C/min. Tensile test was conducted on a WD-II material test system at a strain rate of 1×10^{-3} s^{-1} at room temperature.

3. Results and discussion

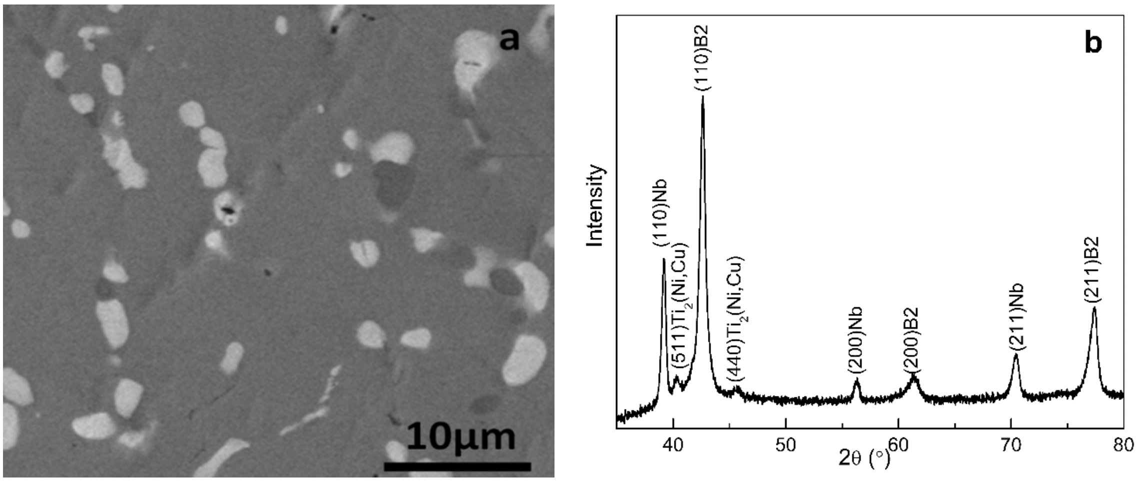

Fig. 1 Microstructure characteristics of the as-cast alloy. (a) SEM back scattered electron micrograph. (b) XRD pattern.

Fig. 1 shows the microstructure characterization of the as cast alloy. The SEM micrograph in Fig. 1a shows that the alloy is consisting of gray area and bright area. The bright area and dark area are confirmed to be Nb-rich phase and TiNiCu respectively by the EDS analysis. Fig. 1b reveals that the alloy is mainly composed of a B2 phase with a small amount of Ti_2(Ni,Cu) type phase, which can be identified by the weak reflection of (511) and (440) planes. These precipitates can be seen as the dark blocks in Fig. 1a. In addition to B2 and Ti_2(Ni,Cu) type phases, an additional phase (Nb-rich phase), which has body-centered cubic (bcc) structure was observed in the alloy. Using reflections (200)Nb and (200)B2, the lattice parameters were determined to be 0.3264 nm for the Nb-rich phase and 0.3016 nm for the B2 phase, respectively.

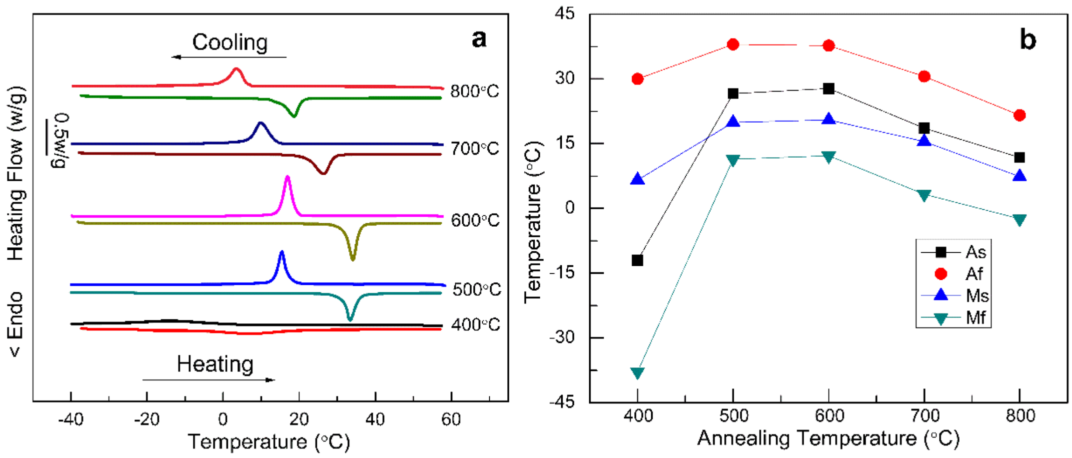

Fig. 2 The transformation behavior of the annealed wire samples. (a) DSC curves upon heating and cooling; (b) Evolutions of phase transformation temperatures with the annealing temperature.

Fig. 2 shows the DSC curves and the corresponding transformation temperatures of the samples annealed at different temperatures for 20 min. All the specimens exhibited direct Austenite (A) to Martensite (M) transformations upon cooling and M-to-A transformations upon heating, which was similar with fully annealed binary near-equiatomic NiTi alloys.

Usually, the TiNiCu alloy with Cu content from 7.5 at.% to 15 at.% showed B2-B19-B19' two-stage transformation [1]. It is believed that this one-step transformation is due to the addition of Nb which suppresses the transformation to B19'. The characteristic temperatures of the transformations were plotted in Fig. 2b as a function of the annealing temperature. It is seen that the transformation temperatures strongly depend on the annealing temperatures. With the increase of the annealing temperature, the transformation temperatures increased to maximum at around 500 °C and 600 °C. This stage corresponds to a dislocation recovery process. The lower transformation temperatures at the initial stage of annealing were attributed to the resistance of high density of dislocations introduced by cold drawing to the lattice distortion of martensitic transformation [11, 12]. The dislocation density decreased with the increasing annealing temperature, therefore the hindered martensitic transformation recovered and occurred at a higher temperature [13]. With further increase of the annealing temperature, the transformation temperatures decreased. The evolution during this stage seems to be related to the grain growth after recrystallization.

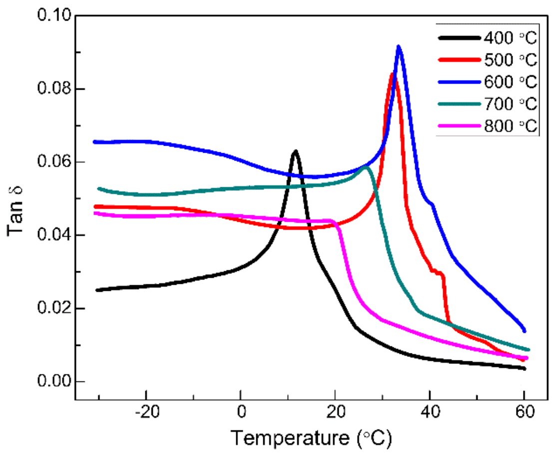

Fig. 3 The damping capacity curve of the annealed samples upon heating.

Fig. 3 shows the damping capacity curve of the annealed samples upon heating. It can be seen that the damping capacity of the martensite and the transformation increased with increasing the annealing temperature first and then decreased. The transformation damping peaks correspond well with the transformation peak on the DSC curves during heating. The samples annealed at 600 °C showed the maximum tan δ of about 0.09. This value is comparable to that of the cold rolled $Ti_{50}Ni_{40}Cu_{10}$ after annealing [14].After annealing at 700 °C and 800 °C, the transformation damping capacity were decreased to almost the same value as the damping capacity of the martensite. These may be due to more precipitates were introduced after high temperature annealing, which will suppress the interface movement of the M/P.

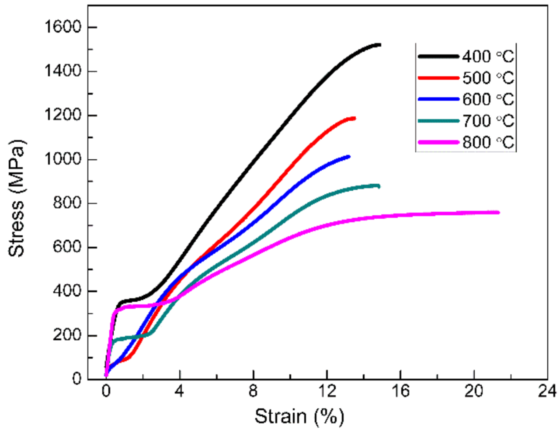

Fig. 4 Tensile stress-strain curves of the annealed alloys.

Fig. 4(a) shows a set of stress–strain curves of the annealed specimens. The specimen annealed at 400 °C exhibited a Lüders-type deformation strain plateau of about 3% with the critical stress for inducing martensitic transformation of about 350MPa. The ultimate strength reaches over 1500 MPa with an elongation of about 14%. Due to the transformation temperature was increased after annealing at 500 °C and 600 °C, they showed lower critical stress of about 50MPa. The elongations of the samples annealed at these temperatures were about 13%. The ultimate strengths were decreased to about 1200MPa and 900MPa, respectively. However, with further increase of the annealing temperature, the critical stress for inducing martensitic transformation increased again to about 150MPa and 320MPa at 700 and 800 °C. The sample after annealing at 800 °C shows the largest elongation over 20%. According to the Clausius–Clapeyron relation [15, 16], the difference between M_s temperature and the testing temperature (300 K) resulted in the progressive evolution of the critical stress for inducing martensitic transformation.

4. Conclusions

This study investigated the microstructure, transformation behavior and mechanical properties of a TiNiCuNb alloy. The addition of Nb made the alloy exhibit only one step B2-B19 transformation upon heating and cooling. Both the transformation temperatures and the damping capacity increased first and then decreased with the increase of the annealing temperature. Meanwhile, the critical stress for stress induced martensitic (SIM) transformation decreased first and then increased with the increase of the annealing temperature. The ultimate strength of the alloy after annealing at 400 °C is over 1500 MPa and the maximum elongation of the alloy after annealing at 800 °C is over 20%.

Acknowledgements

This work was supported by the Australian Research council (Grant No. DP140103805) and the National Natural Science Foundation of China (Grant Nos. 51231008, 51401240, 11474362), the National 973 programs of China (2012CB619403), the Key Project of Chinese Ministry of Education (313055) and Beijing Higher Education Young Elite Teacher Project (YETP0686).

References

[1] T.H. Nam, T. Saburi, K. Shimizu, Mater. Trans. JIM 31 (1990) 959-967.

[2] T.H. Nam, T. Saburi, Y. Kawamura, K. Shimizu, Mater. Trans. JIM 31 (1990) 262-269.

[3] P. Shi, D.Z. Yang, H.M. Shen, F.X. Chen, Materials Des. 21 (2000) 521–524.

[4] G.B. Cho, T.Y. Kim, C.A. Yu, Y. Liu, T.H. Nam, J. Alloys Compd. 449 (2008) 129-133.

[5] Q.Y. Wang, Y.F. Zheng, Y. Liu, Mater. Lett. 65 (2011) 74-77.

[6] G. Cho, T. Kim, T. Nam, C. Yu, Scripta Mater. 53 (2005) 281-285.

[7] K. Uchida, N. Shigenaka, T. Sakuma, Y. Sutou, K. Yamauchi, Mater. Trans. 48 (2007) 445- 450.

[8] M. Piao, S. Miyazaki, K. Otsuka, N. Nishida, Mater. Trans. JIM 33 (1992) 337-345.

[9] H.Y. Kim, T. Jinguu, T. Nam, S. Miyazaki, Scripta Mater. 65 (2011) 846-849.

[10] T. Massalski, “Binary Alloy Phase Diagrams”, 2nd edition, ASM International, Materials Park Ohio, USA, (1990).

[11] X. Ren, N. Miura, J. Zhang, K. Otsuka, K. Tanaka, M. Koiwa, T. Suzuki, Y.I. Chumlyakov, M. Asai Mater. Sci. Eng. A-Struct. 312 (2001) 196-206.

[12] Y. Liu, P.G. McCormick, ISIJ Int. 29 (1989) 417-422.

[13] C.P. Frick, A.M. Ortega, J. Tyber, A.E.M. Maksound, H.J. Maier, Y. Liu, K. Gall, Mater. Sci. Eng. A-Struct. 405 (2005) 34-49.

[14] K.N. Lin, S.K. Wu, Scripta Mater 56 (2007) 589-592.

[15] K.N. Melton, O.Mercier, Acta Metall. 29 (1981) 393-398.

[16] Y. Liu, H. Yang, Smart Mater. Struct. 16 (2007) S22-S27.